RESEARCH ARTICLE

In Vivo Experimental Study on the Effects of Fluid in Increasing the Efficiency of Radiofrequency Ablation

Yi-Xin Sun, Wen Cheng*, Xue Han, Zhao Liu, Qiu-Cheng Wang, Hua Shao

Abstract

Background: Radiofrequency ablation (RFA) is the most widely used and studied method internationally for the local treatment of liver tumors. However, the extension of coagulation necrosis in one RFA procedure is limited and incomplete coverage of the damaged area can lead to a high local recurrence rate. Objective: In this study, we compared the effects of different solutions in enhancing hepatic radiofrequency by establishing a rabbit VX2 liver cancer model. We also determined the optimal solution to maximise effects on the extent of RFA-induced coagulation necrosis. Methods: Thirty VX2 tumor rabbits were randomly assigned to five groups: group A, RFA alone; group B, RFA with anhydrous ethanol injection; group C, RFA with 5% hypertonic saline injection; group D, RFA with lidocaine injection; and group E, RFA with a mixed solution. Routine ultrasound examinations and contrast-enhanced ultrasound (CEUS) of the ablation areas were performed after RFA. Then, we measured the major axis and transverse diameter and compared the areas of coagulation necrosis induced by RFA. Results: The mean ablation area range increased in groups B, C and especially E, and the scopes were greater compared with group A. Preoperative application of anhydrous ethanol, hypertonic saline, lidocaine and the mixed solution (groups B, C, D and E, respectively) resulted in larger coagulation necrosis areas than in group A ($p<0.05$). Among the groups, the coagulation necrosis areas in group E was largest, and the difference was statistically significant compared with other groups ($p<0.05$). Pathological findings were consistent with imaging results. Conclusions: A mixture of dehydrated alcohol, hypertonic saline and lidocaine injected with RFA increases the extent of coagulation necrosis in the liver with a single application, and the mixed solution is more effective than any other injection alone.

Keywords: Ultrasound - radiofrequency ablation - rabbit VX2 tumors - in vivo liver tumor model

Asian Pac J Cancer Prev, **15 (14)**, 5799-5804

Introduction

Hepatocellular carcinoma (HCC) is one of the most common malignant tumors, and is the third leading cause of cancer mortality worldwide (Kamangar et al., 2006; Lee and Liapi, 2009). At present, surgical resection is the most effective method in the treatment when the tumor is restricted to the liver (Achenback et al., 2002; LLovet and Bruix, 2003; Lau and Lai, 2008). However, surgical resection is only possible in a small portion of early HCC patients. Those with advanced liver disease, extra-hepatic metastases, underlying severe liver cirrhosis, inadequate functional hepatic reserves or poor general condition are not eligible for surgery (Bolondi and Gramantieri, 2011; Guo et al., 2012). The limitations of HCC surgical resection have prompted the development of a number of non-surgical therapies, including radiofrequency ablation (RFA), microwave ablation (MWA), percutaneous ethanol injection therapy (PEI), transcatheter arterial chemoembolisation (TACE), high-intensity focused ultrasound (HIFU) therapy, etc.

RFA is the most widely used and most studied method internationally for local treatment (Vallone et al., 2006; Hansler et al., 2007; Peng et al., 2010). RFA can control the entire ablation process via the temperature and impedance control, thereby ensuring the effectiveness and safety of the treatment. However, RFA has limitations: for example, the extension of coagulation necrosis in one RFA procedure is limited. The problem is often attributed to the limitations of tumor size, number, location and other factors. Incomplete formation of the damaged area can lead to a high local recurrence rate. Therefore, improving the range of RFA and reducing the recurrence rate are important problems that need to be solved.

The purpose of this study was to establish the rabbit VX2 liver cancer model and inject anhydrous ethanol, hypertonic saline, lidocaine or a mixed solution to expand the radiofrequency ablation damage zone. Then, we evaluated and compared their effects. We attempted to determine an effective radiofrequency ablation synergistic agent to reduce the incidence rate of single-needle ablation residual carcinomas.

*Department of Ultrasound, The Tumor Hospital of Harbin Medical University, Harbin, China *For correspondence: chengwen69@yahoo.com*

Materials and Methods

The animals

The Animal Ethics Committee of Harbin Medical University, Heilongjiang, China approved this study. All animals were cared for in accordance with Chinese legislation guidelines and the international guidelines on the protection, care and handling of laboratory animals.

In total, 34 New Zealand White rabbits were obtained as recipient animals. Rabbits weighing 2500 - 3000 g were purchased from the Laboratory Animal Centre of The Second Affiliated Hospital of Harbin Medical University. VX2 tumors were implanted and maintained in the thighs of rabbits. The tumors and rabbits were obtained from the laboratory of Shandong Medical University.

Establishment of the rabbit VX2 liver tumor model

VX2 tumors were aseptically resected from the hind limb and minced with surgical scissors and knives in normal saline. The recipient animals were anesthetised using a 3% pentobarbital sodium (1 ml/kg) intravenous ear injection. The abdomen was shaved and prepared with iodine. All inoculations were performed by open laparotomy. To implant the VX2 tumor fragments into the liver parenchyma, a sub-xiphoid laparotomy approximately 3 cm in length was performed to expose the liver lobe following anaesthesia with pentobarbital solution. We used ophthalmic forceps to drill a sinus approximately 5 mm deep in the liver parenchyma and then placed 2-3 pieces of tumor fragments into the sinus. The forceps were removed, and a gelatine sponge was used to seal the sinus to prevent bleeding. All puncture sites were gently compressed for 5 min to prevent leakage of cancer fragments and bleeding from the liver parenchyma. The abdominal incision was then closed in layers. Gentamicin was injected for three consecutive days after laparotomy to prevent infection.

Rabbit VX2 tumor group and treatment

Two weeks later, 32 rabbit VX2 liver tumor models were established, which were identified by ultrasound examination. Two models failed. Two rabbits were randomly selected and sacrificed. The tumor specimens were resected and fixed in 10% formalin liquid for pathological examination". The remaining 30 rabbit VX2 liver tumor models were randomly divided into five groups: group A, RFA; Group B, 1 ml anhydrous ethanol+RFA; group C, 1 ml hypertonic saline+RFA; Group D, 1 ml lidocaine+RFA; and Group E, 1 ml mixed solution (hypertonic saline, lidocaine and anhydrous ethanol)+RFA.

After successfully anesthetising the rabbits, we placed them on the operating table. We used an ultrasound probe to scan each rabbit's liver to determine the tumor position and the suitable needle path. Then, we fixed the probe and used an 18-gauge PTC needle to slowly inject the solution into each lesion. In total, 1 ml of each injection solution was injected up, down, left and right in a four-direction injection. The injection speed was slow (30 seconds).

The Cool-tip RF System (Valley lab, Boulder, CO) consisted of an RF generator (200 W peak power output, 480 kHz electric current), a peristaltic perfusion pump, inflow and outflow tubing, an electrode and a pair of grounding pads. During ablation, the monopole electrode, consisting of a hollow 17-gauge needle with a 1 cm exposed tip, was cooled via an internal circulation of sterile chilled water (4°C). The ablation power was between 15 and 50 W for 4 minutes.

Figure 1. Rabbit VX2 Liver Tumor Mode: General and Pathological Specimens

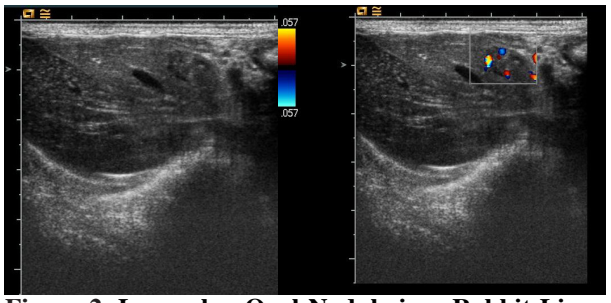

Figure 2. Low-echo, Oval Nodule in a Rabbit Liver. Blood flow signal is evident around the tumor

Ultrasound examination and CEUS

On the 1st, 7th and 14th days after surgery, we used ultrasound to examine and observe the ablation of lesions in the rabbit liver. Moreover, we simultaneously performed contrast-enhanced ultrasound (CEUS) inspections on the 14th day. After successfully anesthetising the rabbits, we placed them on the operating table. A Siemens Sequoia512 colour Doppler ultrasonic diagnostic instrument was used to perform a conventional ultrasound scan of the rabbit liver and aided in our selection of the best scan position. Then, the instrument was converted to imaging mode, and contrast agent (SonoVue, Bracco) was injected at a concentration of 0.1 ml/kg body weight with 2 ml saline flushing. Continuous acquisitions within 3 min dynamic images were stored in the hard drive. The rabbit hepatic angiography phase was divided into the arterial and non-arterial phases (Liu et al., 2012).

Histopathological observation

After CEUS, the rabbits were sacrificed, and the tumor lobe was removed. We made a general observation

Table 1. Comparison of the Average Maximum Ablation Area in Each Group

Group	N	Mean value	Standard deviation	95% confidence interval lower limit	upper limit
RFA	6	91.5	25.952	57.621	125.379
Anhydrous ethanol+RFA	6	328.833	37.247	294.954	362.712
Hypertonic saline+RFA +RFA	6	296	50.947	262.121	329.879
Lidocaine+RFA	6	153	36.764	119.121	186.879
Mixed solution+RFA	6	355.833	45.932	321.954	389.712

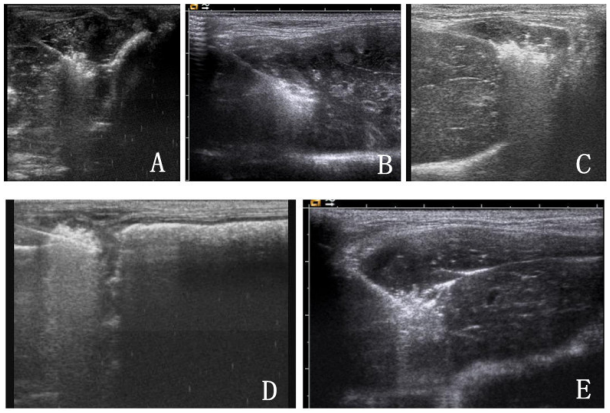

Figure 3. The Performance of Different Groups During Rfa. High-Echo Bubbles were Evident Around the Needle. (A) RFA alone; (B) Anhydrous ethanol+RFA; (C) Hypertonic saline+RFA; (D) Lidocaine+RFA; (E) mixed solution of anhydrous ethanol, hypertonic saline and lidocaine+RFA

regarding tumor morphology after RFA and measured the largest diameter and vertical diameter for comparisons with the imaging measurement results. The specimens were fixed with 10% formalin solution, and haematoxylin and eosin (H&E) staining was performed for pathological observation.

Statistical analysis

Statistical analyses were performed using the SPSS 18.0 statistical software. Differences were considered statistically significant when $p<0.05$.

Results

Animal survival and tumor growth

All of the rabbits underwent RFA therapy using the Cool-tip RF system. No major complications or adverse effects were observed in any of the groups. We did not observe abdominal bleeding, bile fistula or any serious complications, such as abdominal infection. All of the rabbit VX2 liver cancer models of RFA therapy survived for 2 weeks postoperatively and successfully completed CEUS examination before death.

Ultrasound and CEUS of VX2 tumors

zIn the successful intrahepatic-planted models, we observed low- or hypo-echoic nodules with no envelope

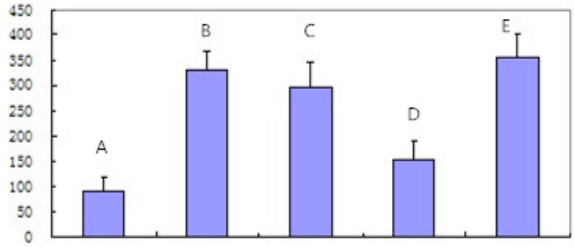

Figure 4. Comparison of the Average Maximum Cross-Sectional Ablation Area in Each Group

and clear borders via ultrasound imaging, along with low-echo haloes surrounding some of the nodules. When necrosis occurred, we observed anechoic areas and scattered and strong echoes inside the nodules. Color Doppler flow imaging indicated the rabbit VX2 liver tumors contained a rich blood supply, which gave priority to peripheral blood. Visible circular or punctiform blood flow signals were evident around the tumors. However, several rabbit VX2 liver tumors were characterised as having little blood supply, and the CDFI blood flow signal was sparse or undetectable.

Experimental rabbits in RFA

During RFA, more obvious strong-echo bubbles were evident around the needles in groups B, C, D and E compared with group A. In the ablation alone group or groups in which the injected solution lacked lidocaine (groups A, B and C), the experimental rabbits displayed a different degree of agitation during the RFA needle electrode burning. The symptoms improved during the pulse interval period. Thus, we hypothesise that a burning pain caused the agitation. In groups D and E, the injected liquid contained lidocaine, so the experimental rabbits were quiet under anaesthesia with no obvious agitation.

Imaging examination after RFA

We did not observe significant differences between the first day and a week after surgery. Using conventional ultrasound, the ablation zone displayed high echo and formed a more irregular, ill-defined boundary between the surrounding normal liver tissue. No blood supply was observed with CDFI. We repeated the ultrasound 14 days later; the ablation area was slightly reduced in size, and the echoes were slightly lower and non-uniform.

Using CEUS, the ablation was not enhanced in central areas in group A after RFA treatment, but the range was smaller. In CEUS, the tissues surrounding the ablation area were characterised by increased echo in the hepatic arterial phase and rapid clearance. The tissues were characterised by low or no enhancement in the non-arterial phase. The tissues contained residual tumor cells upon pathological examination. Group B, C and E tumor ablation areas were not enhanced, and their scopes were greater compared with group A. Group E was the most obvious. However, the shapes of the ablation areas were irregular.

Comparison of the ablation areas two weeks after RFA

Two weeks after RFA, CEUS was performed on the experimental rabbits. We calculated and compared the largest areas of the ablation zones from groups A, B, C,

Table 2. Comparison between Different Groups

(I) group	(J) group	Mean difference (I-J)	Standard error	*P*	95% confidence interval	
					lower limit	upperlimit
RFA	Hypertonic saline+RFA	-204.50*	23.263	0	-252.41	-156.59
	Mixed solution+RFA	-264.33*	23.263	0	-312.25	-216.42
	Lidocaine+RFA	-61.50*	23.263	0.014	-109.41	-13.59
	Anhydrous ethanol+RFA	-237.33*	23.263	0	-285.25	-189.42
Anhydrous ethanol+RFA	RFA	237.33*	23.263	0	189.42	285.25
	Hypertonic saline+RFA	32.83	23.263	0.17	-15.08	80.75
	Mixed solution+RFA	-27	23.263	0.257	-74.91	20.91
	Lidocaine+RFA	175.83*	23.263	0	127.92	223.75
Hypertonic saline+RFA	RFA	204.50*	23.263	0	156.59	252.41
	Mixed solution+RFA	-59.83*	23.263	0.016	-107.75	-11.92
	Lidocaine+RFA	143.00*	23.263	0	95.09	190.91
	Anhydrous ethanol+RFA	-32.83	23.263	0.17	-80.75	15.08
Lidocaine+RFA	RFA	61.50*	23.263	0.014	13.59	109.41
	Hypertonic saline+RFA	-143.00*	23.263	0	-190.91	-95.09
	Mixed solution+RFA	-202.83*	23.263	0	-250.75	-154.92
	Anhydrous ethanol+RFA	-175.83*	23.263	0	-223.75	-127.92
Mixed solution+RFA	RFA	264.33*	23.263	0	216.42	312.25
	Hypertonic saline+RFA	59.83*	23.263	0.016	11.92	107.75
	Lidocaine+RFA	202.83*	23.263	0	154.92	250.75
	Anhydrous ethanol+RFA	27	23.263	0.257	-20.91	74.91

D and E.

In this study, we used a single-factor, completely randomised design analysis of variance to compare the lesion areas of the different groups. The results revealed that F=49.8 (p<0.01), indicating statistically significant differences between the groups. Injections of anhydrous ethanol, hypertonic saline, lidocaine or a mixed solution (B, C, D and E groups, respectively) produced a larger coagulation necrosis area compared with group A (p<0.05). Among these groups, the coagulation necrosis area of group E was the largest. Comparing two groups using the LSD-T test, p<0.05 indicates statistically significant differences.

Discussion

Design of the experimental method The VX2 tumor is a type of squamous cell malignant tumor caused by Shope papilloma viruses (Moore et al., 1959; Sonoda et al., 2011; Tu et al., 2009; Schulz et al., 2008). Extensive research on the biological characteristics of VX2 has identified its characteristics, and its mode of invasion through lymph nodes and blood vessels is very similar to human squamous malignant tumors in head and neck or liver cancer (Ko et al., 2001) . The VX2 tumor is widely used in various animal viscera tumor models and can be vaccinated in rabbit livers, kidneys, muscles, bones and brains, thereby forming tumor animal models in situ (Kuszyk et al., 2000; Ramirez et al., 1995; Geschwind et al., 2000; Larson et al., 2006) . The rabbit VX2 liver tumor model is being increasingly used in experimental studies of liver cancer because the model is easy to establish via an open surgery method and the success rate is high (Hong et al., 2006) . Moreover, the models typically display good stability. Therefore, our study selected the rabbit VX2 liver tumor model given its maximal similarity to human liver, thereby ensuring that the results closely mirrored the clinical research.

In this experiment, each rabbit formed only one focal ablation in the liver. We chose a puncture position far away from the hepatic hilar region to avoid causing too much damage to the rabbit, thereby influencing the rabbit's survival and the experimental effect. When we injected the solution intrahepatically, we controlled the depth of the needle to ensure that the depth was the same every time and that the solution was homogeneous. We injected from four directions: up, down, left and right. The injection speed was slow and controlled and lasted for 30 seconds. The injection volume was 1 ml, which was calculated according to the melting range of the literature and our preliminary experimental results in vitro. The injection of too much liquid can cause excessive solution reflux because the rabbit liver is thin. Moreover, too much liquid easily spreads to normal liver tissues far from the target tissues (Goldberg et al., 2001; Gillams and Lees, 2005) .

When comparing the ablation area, we measured through the needle path across the biggest ablation area section. We measured the length diameter (a) and the vertical diameter (b); we then used the ellipse area formula ($S=\pi ab / 4$) to calculate the cross-sectional area for each group to minimise the error.

Relationship between the injected solution and the RFA range. During RFA, the electrode temperature rises quickly, and the electrode tip can carbonise the surrounding tissue. Thus, the conduction of the electric current during RFA was limited in the organization, and hence the melting ranges were limited. When anhydrous ethanol is injected into the lesions, cell membrane

permeability increases with increasing temperatures. In addition, anhydrous ethanol infiltration within tumor cells can directly kill the tumor. At the same time, the existing experimental results indicated that the thermal loss effect caused by blood perfusion is the major factor that affects the melting range. Some scholars performed experiments demonstrating that decreased blood flow and perfusion could reduce heat loss, improving the scope of the radiofrequency ablation. Ethanol can aid in the identification of micro-vascular thrombosis within the tumor, which can effectively reduce heat loss caused within the tumor via blood perfusion (Zhang et al., 2008). In addition, a study found that the RFA needle electrode-induced carbonisation of surrounding tissues impedes the organization around the needle. This process prevents heat transmission to surrounding tissues and further distances, thus affecting the melting range. Therefore, we thought that when using PEI-RFA, the temperature would gradually rise along with the effect of RFA. The boiling point of ethanol is 78 ºC, and then ethanol is vaporised. The temperature of the tissues surrounding the needle was maintained at 78 ºC, and the temperature increased again until the ethanol completely vaporised. Thus, PEI - RFA delayed tissue carbonisation and improved the melting range (Kuang et al., 2009).

With RFA alone, the melting range is limited (Ji and Xu, 2011; Dai et al., 2012; Hofer et al., 2008). When we injected 5% hypertonic saline, lidocaine or a mixed solution, increased ion concentrations were noted in the ablation areas. At the same time, the cooling effects of the liquid itself reduced the local temperature and delayed organization heating. The use of a solution as a heat conduction medium could promote heat diffusion in the organization; thus, the ablation melting range increased significantly. This technique could reduce the impedance of the organization or could cause the impedance to slow down.

In this study, we used a single-factor, completely randomised design analysis of variance to compare the lesion areas of the different groups. The results indicated statistically significant differences between the groups. Injections of anhydrous ethanol, hypertonic saline, lidocaine and a mixed solution (B, C, D and E groups, respectively) produced larger coagulation necrosis areas compared with group A ($p<0.05$). These solutions imparted beneficial effects on RFA. Among the groups, the coagulation necrosis area of group E was the largest. This phenomenon indicates that the mixture of anhydrous ethanol and hypertonic saline solution has a synergistic effect on RFA. This finding may be attributed to the fact that the sodium chloride and lidocaine solution improved the conductivity of the organization and that anhydrous ethanol promotes micro-thrombosis. The three types of solutions promoted dispersion within the organization and thus reduced heat loss from the organization caused by blood perfusion.

At present, academics have used anhydrous ethanol in RFA therapy for liver cancer and have reported good curative effects. However, most patients may feel pain intra-operatively or postoperatively after anhydrous ethanol injection. In this study, the synergistic agent contains lidocaine, an anaesthesia drug that effectively relieves pain and increases ion concentrations around the needle electrode, thus improving the therapeutic effect.

Using the LSD-T test to compare groups, the differences in group E (mixture) and group B (anhydrous ethanol group) were not statistically significant ($p>0.05$). In addition, no statistically significant differences ($p>0.05$) between group B (anhydrous ethanol group) and group C (hypertonic saline group) were observed. This result may be attributed to the following aspects: (1) at the same temperature, the efficiencies of anhydrous ethanol and hypertonic saline are similar; (2) the mixed solution contains anaesthetic lidocaine and anhydrous ethanol, which may reduce the ionic conductivity compared with other groups; (3) this study used 6 experimental rabbits in each group, and the sample size was smaller. Errors might be present in the sample mean; thus, it cannot accurately reflect the overall situation.

Analysis of imaging findings. The pathological manifestations and transfer methods of rabbit VX2 liver tumors are similar to human liver cancer. VX2 tumors promote increased vascular hyperplasia from artery tumors given their secretion of vascular growth factors. Nourishing blood vessels formed on the base of the artery of tumor (Szala and Jarosz, 2011). Changes in liver tumor haemodynamics led to changes in the ultrasonic imaging phase. Therefore, VX2 and human liver cancers display similar images of the perfusion process, consistent with the VX2 tumor ultrasound imaging in our experiment.

After RFA, the tumor displayed coagulation necrosis, and the CEUS images without enhancement indicated that the local necrotic area lacked a micro-vascular supply. We observed abnormal increases in the internal and surrounding areas in group A; according to CEUS, these areas were characterised as half-ring or nodular. These observations were consistent with the pathological findings. Thus, CEUS can accurately identify the necrosis area and residual tumors and has obvious advantages compared with ordinary ultrasound.

However, similarities and differences between the inflammatory reaction surrounding the ablation zone and residual tumors were evident in the CEUS enhancement patterns. Pei et al. (2006) suggested that the patterns corresponded with inflammatory hyperaemia. Upon pathological examination, the tissues surrounding the ablation zone displayed a 1-2 mm thin circle, which displayed high enhancement in the hepatic arterial phase and equal enhancement in the non-arterial phase. This pattern was different from the enhancement pattern of residual tumors. This observation may occur because SonoVue is a micron-grade contrast agent that cannot permeate the vascular endothelial cells in the blood vessels outside the gap. Inflammatory hyperaemia could be slightly increased compared with the normal tissues due to the expansion of the blood vessels, but this phenomenon would not disappear quickly.

In this experiment, the images of complete ablation areas with peripheral inflammatory cells or fibres in groups B, C and E did not display obvious differences compared with normal liver parenchyma after RFA. This finding is most likely due to differences in the timing of

CEUS. In our experiment, CEUS imaging was performed 2 weeks after the surgery to compare the ablation ranges. The early inflammatory reaction hyperaemia area was fibrotic, and granulation tissue formation had occurred; thus, the inflammatory expansion of local blood vessels was not obvious. Therefore, these findings were consistent with the liver parenchyma imaging performance. In addition, the tumor ablation areas in groups A and D were relatively small; thus, residual tumor cells were present. The presence of residual tumors in the arterial and non-arterial phases was consistent with literature reports.

Several limitations inherent in the study should be noted. First, when the solutions were injected, we noted that the ablation area became irregular in terms of the range of enlargement. This observation may be associated with the uneven dispersion of the solution. Most of the injected fluid concentrated around the lesion centre or needles, and some areas far away from the central organization had less or no liquid distribution. Therefore, this experimental method needs to be further perfected and improved. Second, we only performed the experiments using a single concentration of the solution based on preliminary experimental results and literature reports. The experimental results with other concentrations are not yet clear. Additional experimental studies on the effects of different solution concentrations should be performed.

Acknowledgements

This study is funded by China Heilongjiang province natural science fund (NO. D201170). The authors have no conflicts of interest to declare.

References

Achenbach T, Seifert JK, Pitton MB, Schunk K, Junginger T (2002). Chemoembolization for primary liver cancer. *Eur J Surg Oncol*, **28**, 37-41.

Bolondi L, Gramantieri L (2011). From liver cirrhosis to HCC. *Intern Emerg Med*, **6,** 93-8.

Dai X, Zhao H.-Q, Liu R-H, et al (2012). Percutaneous radiofrequency ablation guided by contrast-enhanced ultrasound in treatment of metastatic hepatocellular carcinoma after liver transplantation. *Asian Pac J Cancer Prev,* **13**, 3709-12.

Geschwind JF, Artemov D, Abraham S, et al (2000). Chemoembolization of liver tumor in a rabbit model: assessment of tumor cell death with diffusion-weighted MR imaging and histologic analysis. *J Vasc Interv Radiol*, **11**, 1245-55.

Gillams AR, Lees WR (2005). CT mapping of the distribution of saline during radiofrequency ablation with perfusion electrodes. *Cardiovasc Intervent Radiol*, **28**, 476-80.

Goldberg SN, Ahmed M, Gazelle GS, et al (2001). Radio-frequency thermal ablation with NaCl solution injection: effect of electrical conductivity on tissue heating and coagulation-phantom and porcine liver study. *Radiology*, **219**, 157-65.

Guo CL, Yang HC, Yang XH, et al (2012). Associations between infiltrating lymphocyte subsets and hepatocellular carcinoma. *Asian Pac J Cancer Prev*, **13**, 5909-13.

Hansler J, Frieser M, Tietz V, et al (2007). Percutaneous radiofrequency ablation of liver tumors using multiple saline-perfused electrodes. *J Vasc Interv Radiol*, **18**, 405-10.

Hofer S, Oberholzer C, Beck S, Looser C, Ludwig C (2008). Ultrasound-guided radiofrequency ablation (RFA) for inoperable gastrointestinal liver metastases. *Ultraschall Med*, **29**, 388-92.

Hong K, Khwaja A, Liapi E, et al (2006). New intra-arterial drug delivery system for the treatment of liver cancer: preclinical assessment in a rabbit model of liver cancer. *Clin Cancer Res*, **12**, 2563-7.

Ji Q, Xu Z, Liu G, et al (2011). Preinjected fluids do not benefit microwave ablation as those in radiofrequency ablation. *Acad Radiol*, 18, 1151-8.

Kamangar F, Dores GM, Anderson WF (2006). Patterns of cancer incidence, mortality, and prevalence across five continents: defining priorities to reduce cancer disparities in different geographic regions of the world. *J Clin Oncol*, **24**, 2137-50.

Ko YH, Pedersen PL, Geschwind JF (2001). Glucose catabolism in the rabbit VX2 tumor model for liver cancer: characterization and targeting hexokinase. *Cancer Lett*, **173**, 83-91.

Kuang M, Lu MD, Xie XY, et al (2009). Ethanol ablation of hepatocellular carcinoma up to 5.0 cm by using a multipronged injection needle with high-dose strategy. *Radiology*, **253**, 552-61.

Kuszyk BS, Boitnott JK, Choti MA, et al (2000). Local tumor recurrence following hepatic cryoablation: radiologic-histopathologic correlation in a rabbit model. *Radiology*, **217**, 477-86.

Larson AC, Rhee TK, Deng J, et al (2006). Comparison between intravenous and intra-arterial contrast injections for dynamic 3D MRI of liver tumors in the VX2 rabbit model. *J Magn Reson Imaging*, **24**, 242-7.

Lau WY, Lai EC (2008). Hepatocellular carcinoma: current management and recent advances. *Hepatobiliary Pancreat Dis Int*, **7**, 237-57.

Lee K-H, Liapi E, Buijs M, et al (2009). Percutaneous US-guided implantation of Vx-2 carcinoma into rabbit liver: A comparison with open surgical method. *J Surg Res*, **155**, 94-9.

Liu Y, Ren W, Liu C, et al (2012). Contrast- enhanced ultrasonography of the rabbit VX2 tumor model: analysis of vascular pathology. *Oncol Lett*, **4**, 685-90.

Llovet JM, Bruix J (2003). Systematic review of randomized trials for unresectable hepatocellular carcinoma: chemoembolization improves survival. *Hepatology*, **37**, 429-42.

Moore DH, Stone RS, Shope RE, Gelber D (1959). Ultrastructure and site of formation of rabbit papilloma virus. *Proc Soc Exp Biol Med,* **101**, 575.

Pei X, Li A, Liang H, et al (2006). Contrast-enhanced ultrasonographic assessment on radiofrequency ablation in rabbit hepatic VX2 tumors. *Chinese J Ultrasound Med*, **22**, 573-6.

Peng ZW, Zhang YJ, Chen MS, et al (2010). Radiofrequency ablation as first-line treatment for small solitary hepatocellular carcinoma: long-term results. *Eur J Surg Oncol*, **36**, 1054-60.

Ramirez LH, Julieron M, Bonnay M, et al (1995). Stimulation of tumor growth *in vitro* and *in vivo* by suramin on the VX2 model. *Invest New Drugs*, **13**, 51-3.

Schulz S, Haussler U, Mandic R, et al (2008). Treatment with ozone/oxygen-pneumoperitoneum results in complete remission of rabbit squamous cell carcinomas. *Int J Cancer*, **122**, 2360-7.

Sonoda A, Nitta N, Nitta-Seko A, et al (2011). Time-course studies of implanted Rabbit VX2 Liver tumors to identify the appropriate time for starting hepatic arterial embolization in animal models. *Oncology*, **80**, 92-6.

Szala S, Jarosz M (2011). Tumorblood vessels. *Postepy Higiene Med Dosw*, **65**, 437-46.

Tu M, Xu L, Wei X, et al (2009). How to establish a solitary and localized VX2 lung cancer rabbit model? A simple and effective intrapulmonary tumor implantation technique. *J Surg Res*, **154**, 284-92.

Vallone P, Catalano O, Izzo F, Siani A (2006). Combined ethanol injection therapy and radiofrequency ablation therapy in percutaneous treatment of hepatocellular carcinoma larger than 4 cm. *Cardiovasc Intervent Radiol*, **29**, 544-51.

Zhang YJ, Liang HH, Chen MS, et al (2008). Hepatocellular carcinoma treated with radiofrequency ablation with or without ethanol injection: a prospective randomized trial. *Radiology*, **246**, 599-607